Simple Metrics Derivation for a Discrete Time Continuous Phase Modulation Receiver

Francisco A. Monteiro, António J. Rodrigues
Instituto de Telecomunicações / Instituto Superior Técnico, Technical University of Lisbon
Av. Rovisco Pais, 1049-001 Lisbon, Portugal
Tel: +351 218418487; Fax: +351 218418472; E-mail: frmo@lx.it.pt

Abstract

This paper presents a practical quasi-optimum full digital receiver for a particular class of continuous phase modulation (CPM). The first step is the sampling of the received signal. Afterwards, only digital signal processing (DSP) is made. The detection process is composed of two software tasks: Viterbi maximum likelihood sequences detection (MLSD) preceded by phase transition metrics calculation.
It is presented a low complexity procedure for metric calculations suitable for schemes having a number of CPM states S=0 mod 4 (S≥4). Those schemes exhibit certain symmetries on the plan of complex phase transitions that allow metric derivations from the metrics of transitions initiating in first quadrant states. ¾ of the metrics are derived by a copy and paste formula, substituting discrete time integrations. As well, metrics of the Q branch can be derived from the I ones. Therefore, a reduction factor of 4×2 can be accomplished for the number of stored transitions and the number of metrics computations.

Key Words

CPM, MLSD, DSP, metrics relations.

1. Introduction

Non-linear amplification is a major problem in wireless systems, causing the called *spectrum re-growth,* which eliminates most of the previous filtering actions. Continuous phase modulation (CPM) signals have constant amplitude and so their insensibility to non-linear amplification makes them an ideal solution; no information is lost for that reason. Also, its phase continuity allows good spectral performance and implies a code gain due to the inherent memory effect. Although those rather good characteristics, its applications are still constrained to few and expensive fixed microwave links. Since early times (20 years now [1]), what is restraining CPM widespread use is its detection complexity. Nowadays, the design of simple receivers is the main focus of attention [2-4].
It will be presented an algorithm that allows an easy software implementation of metrics computations appropriated for a digital signal processing (DSP) maximum likelihood detector. Following the usual baseband conversion and a continuous to discrete time change, all the detection processing is made numerically over those samples. The minimized required data structure is suitable for maximum likelihood sequences detection (MLSD) supported by adaptable tables like the ones in [4].

2. CPM signals

2.1 Signal formatting

A CPM signal is obtained by:

$$s(t,\boldsymbol{\gamma}) = \sqrt{2E_s/T_s}\cos(\omega_c t + \varphi(t,\boldsymbol{\gamma}) + \varphi_0) \qquad (1)$$

The carrier frequency is f_c (ω_c=2πf_c), φ_0 is the arbitrary initial phase and E_s is the energy per symbol, related with the bit energy by E_s=log$_2$(M)·E_b. Channel symbols are $\gamma_i \in \{\pm 1, \pm 3, \cdots, \pm M\text{-}1\}$, forming the M-ary sequence $\boldsymbol{\gamma}$. Each symbol γ_i carries log$_2$(M) bits as a result of a natural mapping of the information bits stream $\boldsymbol{\alpha}$ (example in Table 1).

Table 1: Natural mapping for 8-CPM.

$\{\alpha_i\}$	000	001	010	011	100	101	110	111
γ_i	-7	-5	-3	-1	+1	+3	+5	+7

The information carried by N_s channel symbols is keyed in signal's phase as

$$\varphi(t,\boldsymbol{\gamma}) = 2\pi h \sum_{i=0}^{N_s} \gamma_i q(t - iT_s) \qquad (2)$$

A constant modulation index, h=p/q, is considered, where p and q are integers having no common factors. The phase transition pulse shape, $q(t)$, affects phase transitions during L symbols (L>1 for partial response signalling). $q(t)$ is defined by the frequency pulse shape, $g(t)$:

$$q(t) = \int_{-\infty}^{t} g(\tau)\,d\tau \qquad (3)$$

The normalisation $q(t) = \int_0^{\infty} g(\tau)\,d\tau = 1/2$ is applied so that the maximum phase transition during a symbol time, T_s, is h·(M-1)·π. In general, φ_i evolve $h\cdot\gamma_i\cdot\pi$ within T_s.
Different frequency pulses define distinct CPM

families. The most common are: LREC (rectangular), LRC (raised cosine) and the popular GMSK (gaussian minimum shift keying). The first is defined by

$$g(t) = \frac{1}{2}\text{rect}\left(\frac{t - LT_s}{LT_s}\right) = \begin{cases} \dfrac{1}{2LT_s}, & 0 \le t \le LT_s \\ 0 \quad , \text{elsewhere} \end{cases} \tag{4}$$

When L=1 it's also known as continuous phase frequency shift modulation (CPFSK). From (1), (2) and (4), CPFSK signals can be expressed as

$$s(t,\boldsymbol{\gamma}) = \sqrt{2E_s/T_s}\cos\{2\pi[f_c t + 1/2\,\gamma_i h\cdot(t/T_s - i)] + \varphi_i\}, \quad iT_s \le t \le (i+1)T_s \tag{5a}$$

$$\varphi_i = h\pi\sum_{i=-\infty}^{i-1}\gamma_i \mod 2\pi \tag{5b}$$

CPFSK embodies great importance since it lower bounds what we can expect from a set of h and M, remembering that smother pulse shapes will allow better spectrum efficiency [1]. Larger M and shorter phase transitions (smaller h) also produce band narrowing. L>1 improves power efficiency.

In CPFSK different frequencies can be detected during each T_s. Minimum shift keying (MSK) and Sünde's BFSK are particular cases with h=1/2 and h=1, respectively.

2.2. CPM performance

In order to evaluate performance one uses the *minimum Euclidean distance* between two signals transporting respectively the symbols sequences $\boldsymbol{\gamma}$ and $\boldsymbol{\gamma}'$:

$$D^2_{\min}(\boldsymbol{\gamma},\boldsymbol{\gamma}') = \min_{\boldsymbol{\gamma},\boldsymbol{\gamma}':\boldsymbol{\gamma}\neq\boldsymbol{\gamma}'}\int_0^\infty [s(t,\boldsymbol{\gamma}) - s(t,\boldsymbol{\gamma}')]^2\,dt \tag{6}$$

It is useful to define the *minimum normalised squared Euclidean distance* (MNSED) as

$$d^2_{\min}(\boldsymbol{\gamma},\boldsymbol{\gamma}') = \frac{D^2_{\min}(\boldsymbol{\gamma},\boldsymbol{\gamma}')}{2E_s} \tag{7}$$

Using trigonometry, it can be showed [5-Sec.2.2.3] that

$$d^2_{\min}(\boldsymbol{\gamma},\boldsymbol{\gamma}') = \frac{\log M}{T_s}\min_{\boldsymbol{\gamma},\boldsymbol{\gamma}':\boldsymbol{\gamma}\neq\boldsymbol{\gamma}'}\int_{iT_s}^{(i+1)T_s}[1 - \cos(\varphi(t,\boldsymbol{\gamma}) - \varphi(t,\boldsymbol{\gamma}'))]^2\,dt \tag{8}$$

MNSED can be interpreted as a cumulative sum of *incremental normalised Euclidean distances*, d_i, defined over each one of the N_s symbols:

$$d^2_{\min} = \sum_{i=0}^{N_s-1} d_i^2 \tag{9}$$

Optimum CPM detection, presented in Section 2.2., is based on this property. Therefore, from (6), (7) and (9)

$$d_i^2 = \frac{1}{2E_s}\min_{\boldsymbol{\gamma},\boldsymbol{\gamma}':\boldsymbol{\gamma}\neq\boldsymbol{\gamma}'}\int_{iT_s}^{(i+1)T_s}[s(t,\boldsymbol{\gamma}) - s(t,\boldsymbol{\gamma}')]^2\,dt \tag{10}$$

The bit error rate (BER) is, e.g. [5-p.55]:

$$P_b \approx C\cdot Q\left(\sqrt{d^2_{\min}\frac{E_b}{N_0}}\right) \approx Q\left(\sqrt{d^2_{\min}\frac{E_b}{N_0}}\right) \tag{11}$$

C is a constant dependent on the signal space (≈1 in CPM). $Q(x)$ is the area under the unit variance gaussian probability distribution in $[x, \infty]$. Notice that power efficiency comparisons can be made merely by $d^2_{\min}$ knowledge.

3. MLSD detection

3.1. Problem statement

At the edges of every interval, phase $\varphi(t,\boldsymbol{\gamma})$ always lies in one of the following cases:

$$\varphi_i \in \{0,\ \pi p/q,\ 2\pi p/q,\cdots,\ (q\text{-}1)\pi p/q\}\ \text{, for even } p \tag{12a}$$

$$\varphi_i \in \{0,\ \pi p/q,\ 2\pi p/q,\cdots,\ (2q\text{-}1)\pi p/q\}\ \text{, for odd } p \tag{12b}$$

CPM states are defined by the sets

$$S_i = \{\varphi_i, \gamma_{i\text{-}1}, \gamma_{i\text{-}2}, \cdots, \gamma_{i\text{-}L+1}\} \tag{13}$$

The number of states is then

$$S = q\cdot M^{L\text{-}1}\ \text{, for even } p \tag{14a}$$

$$S = 2q\cdot M^{L\text{-}1}\ \text{, for odd } p \tag{14b}$$

For a total response system (L=1), S corresponds to the number of physical phase states. Writing the modulation index in the form h=2k/q (k and q as in section 2.1) the number of states is given only by $S = q\cdot M^{L\text{-}1}$.

Fig. 1 depicts two possible representations for CPM with M=2 and h=1/2 – S=4 from (14b) –, i.e. MSK, being φ_0=0.

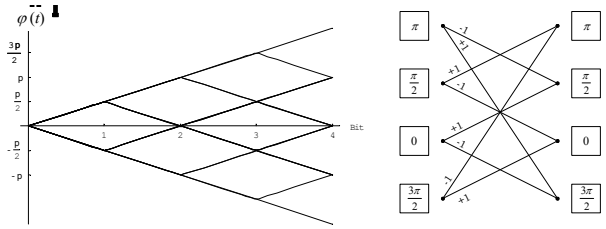

(a) Phase tree. (b) Phase trellis.

Figure 1: MSK representations (φ_0=0).

Departing from each state one has M different branches, so, there are

$$\Xi = S\cdot M \tag{15}$$

phase transitions denoted by

$$\boldsymbol{\tau}_b = \varphi(t,\gamma_m) = \gamma_m\cdot h\cdot q(t),\ b = 1, 2, \cdots, \Xi \tag{16}$$

where $m = b - (M\times$("*state #*"-1)). This relation will be better explained in section 4.

From (14b), the number of branches for an odd p is

$$\Xi = 2q\cdot M^L \tag{17}$$

3.2. Optimum detection

The optimum CPM receiver for a signal $y(t)$, corrupted

by additive white gaussian noise (AWGN), $n(t)$, i.e.:

$$y(t,\boldsymbol{\gamma}) = s(t,\boldsymbol{\gamma}) + n(t) \tag{18}$$

is achieved using maximum likelihood sequence detection (MLSD) principles. It consists of a metrics calculation block followed by a Viterbi decoder. The optimum likelihood metric is the MNSED, $d^2_{\min}$. For the transitions $\tau_b(t)$, for b=1, 2, ···, Ξ, they are:

$$\Lambda_b = d^2_{\min}\left(y_i(t) = y(t,\gamma_i),\ \tau_b(t) = s(t,\gamma_m)\right) \tag{19}$$

which are calculated from

$$\begin{aligned} d^2_{\min}(y_i,\tau_b) &= \left\|y(t,\gamma_i), s(t,\gamma_m)\right\|^2 = \\ &= \left\|y(t,\gamma_i)\right\|^2 + \left\|s(t,\gamma_m)\right\|^2 - 2\left\langle y(t,\gamma_i), s(t,\gamma_m)\right\rangle \\ &= E_{y,i} + E_{\tau,b} - 2\left\langle y(t,\gamma_i), s(t,\gamma_b)\right\rangle \end{aligned} \tag{20}$$

The index i is associated to the i^{st} transmitted symbol and b is associated to the Ξ possible transitions τ_b. The energy of the received symbol, E_{yi}, is independent of the transition and, as well, the energies of the possible symbols are all the same ($E_{\tau,b}$=E_s) – see (1). Therefore, the metrics yield in the inner product:

$$\Lambda_b = \left\langle y(t,\gamma_i), \tau_b(t) = s(t,\gamma_m)\right\rangle \tag{21}$$

When using (21) instead of (19), MLSD must search the sequence $\boldsymbol{\gamma}$ having maximum metric and not the minimum.

Metrics can be acquired by Ξ correlators or matched filters. That number is often unbearable for practical use. Fig. 2 shows a metric computation cell (MCC) for optimum detection after additive white gaussian noise (AWGN). This MCC is to be used successively Ξ times during a time symbol to be equivalent to the structure of parallel correlators. During symbol i, the MCC must be used for all transitions $\tau_{I,b} \in \{\tau_{I,1}, \tau_{I,2}, \cdots, \tau_{I,\Xi}\}$ and all $\tau_{Q,b} \in \{\tau_{Q,1}, \tau_{Q,2}, \cdots, \tau_{Q,\Xi}\}$.

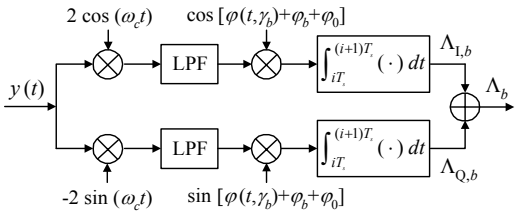

Figure 2: Metric computation cell (MCC).

It should be remembered that, after baseband conversion,

$$\begin{aligned} \Lambda_b &= \int_{T_s} y_i(t)\exp(j\varphi(t,\gamma_b))\,dt = d^2_{I,b} + d^2_{Q,b} \\ &= \int_{T_s} y_{I,i}(t)\tau_{I,b}(t)\,dt + \int_{T_s} y_{Q,i}(t)\tau_{Q,b}(t)\,dt \end{aligned} \tag{22}$$

For a zero-order symbol-by-symbol detection the procedure is:

$$\hat{\gamma}_i = \max_b(\Lambda_b), \quad b=1, 2, \cdots, \Xi \tag{23}$$

Unlike this simple detection, MLSD with a Viterbi detector implies great complexity especially when high M and/or weak modulation indices are used to enhance spectrum behaviour, causing an increase in S. During Viterbi algorithm execution one can take in account that S can be cut in half. For the chosen phase transitions (odd γ_i), phase states can be classified in two classes: *odd states* ($\{1\pi p/q,\ 3\pi p/q, \cdots,\ (2q\text{-}1)\pi p/q\}$) and *even states* ($\{0,\ 2\pi p/q, \cdots, (2q\text{-}2)\ \pi p/q\}$) – see Fig. 4 ahead. When a symbol interval ends, the possible state belongs to just one of those two classes (of S/2 states).This simplification cannot be applied to detect a multi-h CPM scheme due to its time variant trellis.

3.3. Proposed receiver

In the proposed receiver a full discrete time processing, preceded by sampling, replace the traditional bench of matched filters. Fig. 3 shows the overall receiver structure. In this section the analysis will assume ideal synchronism recovery.

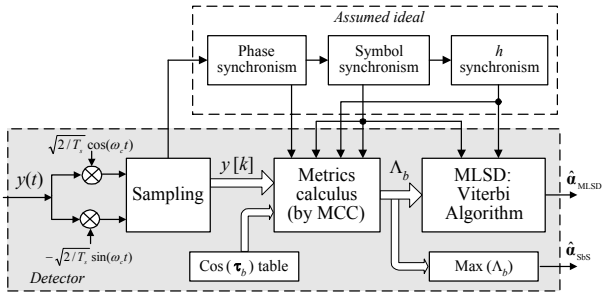

Figure 3: Proposed receiver (the extraction for symbol-by-symbol detection is also depicted).

Being K_s the number of samples per symbol, the sampling period is

$$T_a = T_s / K_s \tag{24}$$

The detector is optimum for the sampled signal $y[k]$= $y(kT_a)$. The sampling rate determines the asymptotical optimality.

Discrete time transitions form the lines of matrix $\mathbf{T}$, i.e,

$$\begin{aligned} &\mathbf{T} = \left[\ \boldsymbol{\tau}_1[k], \boldsymbol{\tau}_2[k], \cdots, \boldsymbol{\tau}_\Xi[k]\ \right]^T \Leftrightarrow \\ &\mathbf{T}(b,k) = \boldsymbol{\tau}_b[k], \quad k=1, 2, \cdots, K_s \end{aligned} \tag{25}$$

being the stored transitions

$$\boldsymbol{\tau}_b[k] = h\cdot\gamma_m\cdot q[k], \quad k=1, 2, \cdots, K_s \tag{26}$$

(m was defined at the end of 3.1.)

In base-band, the proposed detector makes use of

$$\boldsymbol{\tau}_{I,b} = \cos(\boldsymbol{\tau}_b) \tag{27a}$$

$$\boldsymbol{\tau}_{Q,b} = \sin(\boldsymbol{\tau}_b) \tag{27b}$$

These vectors constitute matrixes $\mathbf{T}_I$ and $\mathbf{T}_Q$ (both size $\Xi\times K_s$). It shall be shown in the next section that only

phase transitions $\boldsymbol{\tau}_{I,b}$, for b =1, 2, ···, $q/2{\cdot}M = \Xi/4$, are required, i.e, only the first $\Xi/4$ lines of $\mathbf{T}_I$.

4. Metrics derivations

By restraining CPM schemes to those having a number of states S=0 mod 4 ($S \geq 4$), one can reduce memory size and the number of operations. For that class of schemes we can always distribute the states by the four quadrants in a symmetric manner. For that, the initial phase cannot be 0. The best approach is to impose $\varphi_0 = h\pi/2$. This way, the entire set of phase states is rotated and no state can ever lie on an axis ($\mathrm{Re}\{S_i\}$ or $\mathrm{Im}\{S_i\}$=0, being S_i the complex low-pass equivalent phase state). That would bring a non-resoluble ambiguity for correct detection of those states when using the proposed algorithm. Once absolute synchronism is acquired, it is possible to adjust the signal space to the wanted configuration. There are $q/2$ states inside each quadrant.

Just like in the optimum receiver, metrics must be calculated and placed in vector $\boldsymbol{\Lambda}$ of Ξ elements. Taking in consideration the relations between transitions (summarised in Fig. 4) and other trigonometric relations, the data structure sufficient to obtain all the Ξ metrics is just:

-One vector storing the *M* symbols:

$\boldsymbol{\gamma}_\tau$ =[···, -7,-5,-3,-1,+1,+3,+5,+7, ···];

-A table, $\mathbf{T}_I$ with $\Xi/4$ *in phase* transitions, $\boldsymbol{\tau}_{I,b}$.

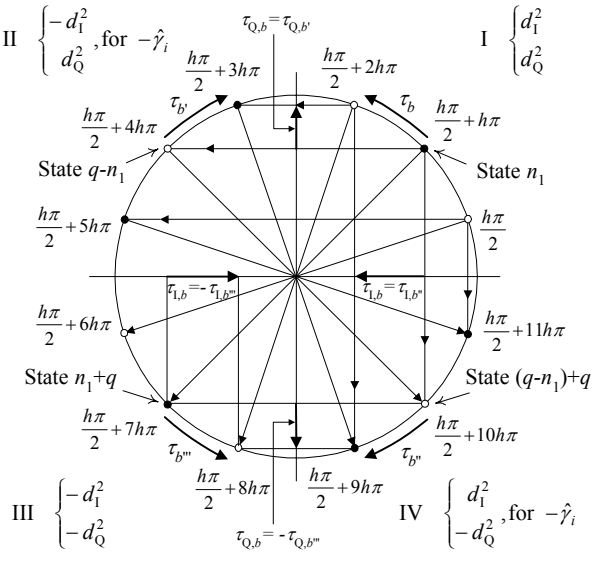

Figure 4: Metrics relations and coping procedures. The example is for h=1/6 (S=12). (*Odd* and *even states* are differentiated.)

The symbols inside $\boldsymbol{\gamma}_\tau$ are γ_m (see 3.3.) being their positions numbered as $\{\gamma_1, \gamma_2, \cdots, \gamma_M\}$. Notation such as $\tau(\gamma_\tau[m])$ refers to a phase transition associated to the symbol of the vector γ_τ in position m. $\tau(\gamma_b)$ denotes exactly the same in a shorter way, remembering that $m=b-(M\times$ ("*state #*"-1)).

For states # n_1=1, 2,···, S, inside quadrants I, II, III and IV, the procedure to obtain all the metrics Λ_b, using the specified data structures, should be:

- Q.I: calculate the metrics for each M transition initiating in each state inside the quadrant I. For each $\mathbf{T}[b=n_1+n_2, k] = \tau(\gamma_\tau[n_2])$, for n_2=1, 2,···, M, calculate:

$$d_{I,b}^2 = \mathbf{y}_i \cdot \left(\boldsymbol{\tau}_{I,b}\right)^T = \sum_{k=1}^{K_s} y[k - iK_s] \cdot \cos\left(\tau_b[k]\right) \qquad (28a)$$

$$d_{Q,b}^2 = \mathbf{y}_i \cdot \left(\boldsymbol{\tau}_{Q,b}\right)^T = \sum_{k=1}^{K_s} y[k - iK_s] \cdot \sin\left(\tau_b[k]\right) \qquad (28b)$$

One can also remember that phase transitions and its sine and cosine functions are related by $\sin(\varphi)=\cos(\varphi - \pi/2)$. For that reason matrix $\mathbf{T}_Q$, containing the transitions signals in quadrature, does not need to be stored. Those transitions already exist inside matrix $\mathbf{T}_I$, each one located precisely $q/2{\cdot}M$ positions before, considering mod Ξ operations. So (28b) can be applied using:

$$d_{Q,b}^2 = \mathbf{y}_i \cdot \left(\boldsymbol{\tau}_{I,b-\frac{q}{2}M \bmod(\Xi/4)}\right)^T =$$

$$= \sum_{k=1}^{K_s} y[k - iK_s] \cdot \cos\left(\tau_{b-\frac{q}{2}M\,(\mathrm{mod}\,\Xi/4)}[k]\right) \qquad (29)$$

Up until now, $\Xi/4$ metrics have been successively calculated and placed inside $\boldsymbol{\Lambda}$ in positions

$$b_I = n_1 + n_2; \qquad (30)$$

Metrics for quadrants II, III and IV will be copied from them in this manner:

- Q.II: Metrics associated to transitions initiating in state number q-n_1 are copied from positions b_I to positions b_{II} for the symmetric symbol of $\boldsymbol{\gamma}_\tau$ (due to the inverse rotations shown in Fig. 4) respecting

$$d_{I,b}^2 = -d_{I,b}^2; \quad d_{Q,b}^2 = d_{Q,b}^2; \qquad (31a,b)$$

$$b_{II} = (q\text{-}n_1)M + (M\text{-}n_2); \qquad (32)$$

(The notation for the I and Q branches partial metrics was established in Fig. 2.)

- Q.III: For states number n_1+q, metrics should be copied from b_I to positions b_{III} respecting

$$d_{I,b}^2 = -d_{I,b}^2; \quad d_{Q,b}^2 = -d_{Q,b}^2 \qquad (33a,b)$$

$$b_{III} = b_{II} + q = n_1 + n_2 + q \qquad (34)$$

- Q.IV: For the state number $(q$-$n_1)+q$, metrics should be copied from b_I to positions b_{IV} respecting

$$d_{I,b}^2 = d_{I,b}^2; \quad d_{Q,b}^2 = -d_{Q,b}^2 \qquad (35a,b)$$

$$b_{IV} = b_{II} + q = (q\text{-}n_1)M + (M\text{-}n_2) + q \qquad (36)$$

In all cases n_2 always runs the cycle n_2=1, 2, ···, M.

Fig. 5 shows the numbering of the transitions positions as a function of the associated state and the relations

between them. Copies are affected by "±" signals depending on quadrants and if it's a $\Lambda_{I,b}$ or $\Lambda_{Q,b}$ metric. The final vector of Ξ metrics, $\mathbf{\Lambda}_i$, stores the sums of those partial metrics, which can be made cumulatively.

In Fig. 4 it is analyzed a case of a transition τ_b in quadrant I. It's possible to see that the *in phase* transition, $\tau_{I,b}$, is the equal to the one of $\tau_{b''}$ in quadrant IV and symmetric of $\tau_{b'}$. Observations of this type are also illustrated for the Q branch.

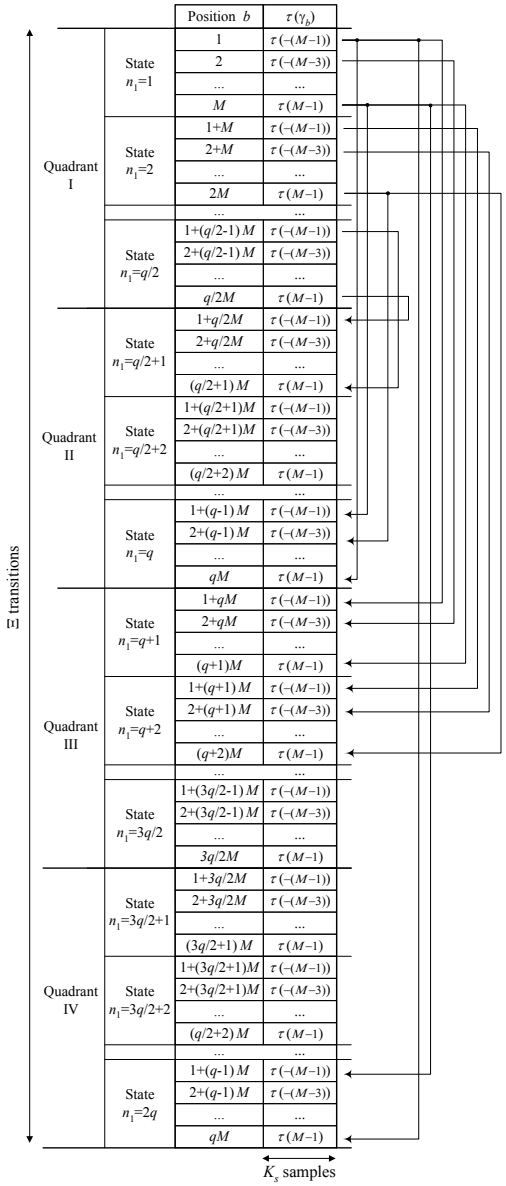

Figure 5: Relation between metrics positions and states.

5. Simulation in AWGN

The receiver was evaluated with AWGN (see 3.2.) by means of computer simulations in *Matlab*, using matrixes and vectors only. The low-pass equivalent is used, thus the receiver deals with signals like the one depicted in Fig. 6(b).

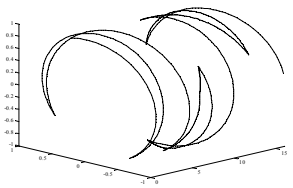

(a) Complex phase evolution.

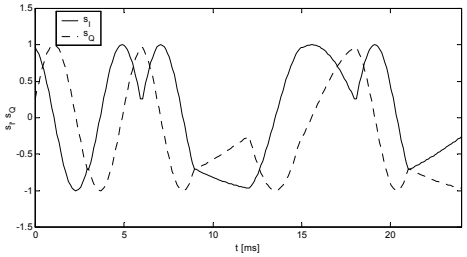

(b) I and Q low-pass equivalent.

Figure 6: Example for a CPFSK sequence of 8 symbols with h=1/6 and M=8, being E_b/N_0=∞.

The receiver is tested for the schemes MSK (M=h=1/2) and M=8, h=1/6 CPFSK (denoted by $M8h61$REC). The goal is not to study these modulations but rather to demonstrate the feasibility of the proposed receiver.

MSK has a MNSED of 2. So, gains over MSK power performance are G=10log($d^2_{\min}$ /2). $M8h61$REC has, indeed, a loss do MSK: G=≈-4dB. ζ_{99} is the spectral efficiency linked to the 99% RF bandwidth, B, and so, ζ=1/(BT_s). MSK has ζ_{99}=0.84 bps/Hz and $M8h61$REC has ζ_{99}≈1.4 bps/Hz (all data extrapolated from [1, 5-p.63]). MSK has S=4 and $M8h61$REC has S=12 (see 3.1 and Fig. 4). $M8h61$REC is not a good scheme by itself in terms of power efficiency. However, concatenated with a convolutional rate 2/3 code, leads to the best known coded CPM system in terms of joint power-bandwidth efficiency and complexity [6-p.246]. That was the motivation to test it.

Fig. 7 presents all the signals stored in $\mathbf{T}_I$ (and the others) for $M8h61$REC. Ξ=96 and only 24 $\tau_{I,b}$ are needed. The other 72 $\tau_{I,b}$ and all the other 96 $\tau_{Q,b}$ can be derived from these. It's possible to see the M=8 transitions starting (and merging) on each state of quadrant I. Note that each line hides two *in phase* transitions.

The first analysis concerns the study of the minimum K_s (Fig. 8), as in (24), so that the power penalty can be small (< 1 dB). For MSK that number is 8 and for $M8h61$REC is 16. Less samples conducts to poor performances in terms of P_b. That results from the greater signal transitions of $M8h61$REC.

Symbol-by-symbol detection based on γ_i were made to show that it's indispensable to take advantage of the memory effect in CPM by MLSD, which enforces an error correction by discarding improbable sequences.

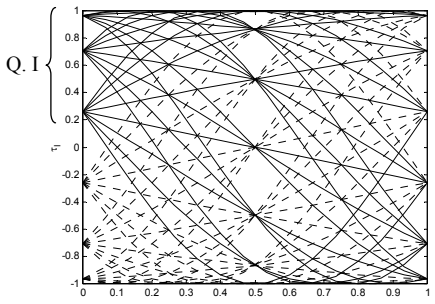

Figure 7: Signals in memory in $\mathbf{T}_I$ for h=1/6, M=8 CPFSK (solid) and the transitions not stored (dashed).

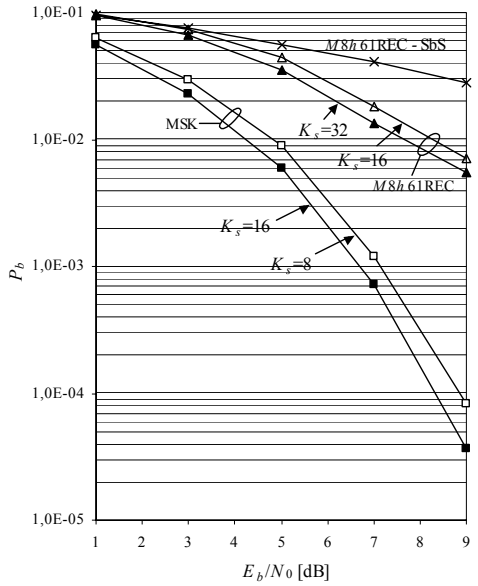

Figure 8: Sampling rate effect for MSK and *M*8*h*61REC.

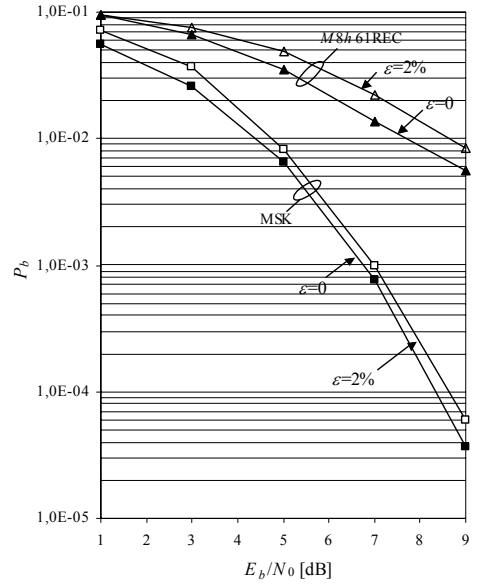

Figure 9: Synchronism error effect for MSK and *M*8*h*61REC (with optimum K_s for each case).

The effect of imperfect phase synchronism is the second test. The phase error is considered in the form

$$\Delta\varphi = 2\pi\varepsilon \tag{37}$$

The results are presented in Fig. 9. It is seen that the phase error induces greater losses in *M*8*h*61REC than in MSK.

6. Conclusions

A quasi-optimum receiver operating on a software radio concept was showed. It can be used for the class of CPM schemes having a number of states multiple of 4. Only transitions metrics associated to transitions emerging from first quadrant must be calculated, and only for the *in phase* branch. All the others metrics (other quadrants and Q ones) are proved to be related to them. Those operations involving discrete integrals are substituted by simple copy/paste procedures of reals.

The optimum receiver needs the storage of 2Ξ transitions so that 2Ξ inner products can be computed (Ξ for I and Ξ for Q analysis) in order to obtain Ξ metrics after each channel symbol. Hence, the reduction factor for memory size and number of integrals is 8.

MSLD results were compared with hard decisions on a symbol-by-symbol basis, showing the gain achieved by the former.

Synchronism is critical due to the assumption of symmetries. The receiver is asymptotically optimum when the sampling rate increases. Note that the sampling procedure is the only factor of non-optimality for the AWGN test case.

7. References

[1] T. Aulin and C. Sundberg, "Continuous Phase Modulation - Part I: Full Response Signalling", *IEEE Trans. on Comm.*, vol. Com-29, no. 3, pp. 196-209, Mar. 1981.

[2] T. Svensson, A. Svensson, "Reduced Complexity Detection of Bandwidth Efficient Partial Response CPM," *in Proc. of IEEE VTC'99*, Houston, Texas, pp. 1296-1300, May 1999.

[3] Weiyi Tang and Ed Shwedyk, "A Quasi-Optimum Receiver for Continuous Phase Modulation", *IEEE Trans. on Comm*, vol. 48, no. 7, pp. 1087-1090, July 2000.

[4] C. J. A. Levita, M. Benaissa and I. J. Wassell, "Adaptable Viterbi Detector for a Decomposed CPM Model Over Rings of Integers", *IEE Proc. Comm.*, vol. 147, no. 3, pp. 137-143, June 2000.

[5] J. Anderson, T. Aulin, C. Sundberg, *Digital Phase Modulation*, Plennum Press, New York, 1986.

[6] Ezio Biglieri, Dariush Divsalar, Peter J. McLane e Marvin K. Simon, *Introduction to Trellis-Coded Modulation with Applications* (Sec. 6.5), Macmillan, 1991.